Research Article

Journal of
Environmental
Nanotechnology

# Optimizing the Tensile and Flexural Properties of Flax/Sisal with $SiO_2$ Nanocomposites Using Response Surface Methodology

M. Vanitha Lakshmi[1], G. Aloy Anuja Mary[2], I. Chandra[3], E. Sivanantham[4] and N. Bharatha Devi[5]*

[1]Department of ECE, School of Engineering, Presidency University, Bangalore, KA, India
[2]Department of ECE, Veltech Rangarajan Dr. Sagunthala R&D Institute of Science and Technology, Avadi, TN, India
[3]Department of CSE, Anna University, Chennai, TN, India
[4]Department of ECE, Rajalakshmi Institute of Technology, Chennai, TN, India
[5]Department of CSE, Saveetha School of Engineering, Saveetha Institute of Medical and Technical Sciences, Saveetha University, Thandalam, TN, India
Received: 25.07.2024 Accepted: 25.09.2024 Published: 30.09.2024
*bharathi.actech@gmail.com

## ABSTRACT

This study aimed to examine the impact of fiber orientation on the tensile and flexural strengths of composites composed of Flax and sisal fibers, particularly at orientations of 0, 45, and 90 degrees. Furthermore, the research sought to determine the most effective parameters for the treatment process. The researchers utilized Response Surface Methodology (RSM) in conjunction with Central Composite Designs (CCD) to develop and analyze their studies. The main objective was to enhance crucial variables such as fiber alignment and the proportions of flax and sisal fibers. Quadratic models were employed in this study to forecast the tensile and bending characteristics of the materials. The best tensile strength (TS) was reached by meticulously experimenting with the fiber orientation and altering the amounts of flax and sisal fibers. The most effective parameter was a fiber orientation of 0 degrees, with a combination of flax and sisal fibers at a concentration of 60 percent each. Under these circumstances, the composite exhibited a significant improvement of 35% in tensile strength and 26% in bending strength when compared to the lowest values achieved with RSM optimization. The notable enhancements demonstrate that aligning the fibers can effectively increase the tensile and flexural strength (FS) and strengthen the bonding between natural fibers and polymer matrix structures.

**Keywords:** Tensile strength; Bending strength; Nano clay; Nanocomposite; RSM.

## 1. INTRODUCTION

The environment strategically aligns reinforcing fibers to form plant structures that can effectively endure external stresses, such as folding caused by wind (Cordin *et al.* 2018). The design of man-made composites was motivated by this natural concept, which then prompted a comprehensive experimental study on the impact of fiber orientation (Mohd *et al.* 2020; Huang *et al.* 2021). Fiber-reinforced polymers typically demonstrate improved characteristics such as reduced weight, resistance to corrosion, and high levels of tensile stress and modulus (Jothi Arunachalam *et al.*2024; Van De Werken *et al.* 2019). Carbon, glass, and aramid fibers are frequently employed as reinforcing in matrices polymers in engineering uses (Arunachalam *et al.* 2024)). Nevertheless, these fibers possess certain disadvantages such as exorbitant manufacturing expenses, recycling complexities, and difficulty managing them after their lifespan (Arunachalam *et al.* 2024). Therefore, the utilization of organically grown fibers to strengthen matrix polymerization has attracted considerable attention in the past decade (Rangasamy *et al.* 2021; Chang *et al.* 2021).

Saravanakumar *et al.* (2024) investigated the anisotropic mechanical characteristics of banana fiber materials by modifying the loading, orientation, and treatment of the fibers using RSM and Artificial Neural Networks (ANN). Zhang and He, (2022) investigated that demonstrates outstanding mechanical characteristics. Incorporating batching normalization and dropout layers improves the model's resilience. The study's findings indicate that the anisotropy of the composite is significantly affected by both the NaOH pre-treatment and the fiber direction.

Manral *et al.* (2023) aimed to construct a model for prediction for three criteria: chemical concentration (CC), treatment duration (TT), and type of mat. The framework was designed to anticipate outcomes based on these factors. The response variables analysed included TS, FS, and IS. The analysis of variance demonstrated that the three-parameter mentioned above had significant individual and interaction effects on the experimental responses. Out of these factors, it was determined that the level of chemicals had the greatest impact on alterations in mechanical characteristics.

Benzannache *et al.* (2021) investigate the impact of treating wood fibers using sodium hydroxide on the mechanical characteristics of the resultant bio composite. The results suggest that adding Wood fibers to the plaster matrix improves both the mechanical strength and flexibility of the composite. The experimental findings were statistically analysed using RSM. The results of the ANOVA analysis reveal that the concentration of sodium hydroxide has a substantial impact on both the TS and FS. The optimization analysis concluded that the most favourable concentration of sodium hydroxide is 20%, and the optimal duration of treatment is 168 hours, which is consistent with the experimental findings.

Iliyasu *et al.* (2022) utilized Deleb palm fiber as a novel reinforcement in epoxy, to improve its physical and mechanical capabilities by leveraging its elemental makeup. The RSM study determined that an Epoxy-Deleb palm fiber composite with a fiber reinforcement content of 40% and a fiber length of 3 mm yielded the most favorable results. This composite demonstrated superior strength in all mechanical parameters, along with a water absorption level of 0.369%. The findings indicated that the unique characteristics of Deleb palm fiber had a substantial impact.

Nugroho and Budiyantoro, (2022) investigated the association between the fiber variables and response variables and were investigated using RSM and ANOVA. The results suggest a significant correlation between the projected response values of the model and the outcomes of the validation test. The FS of the composite was found to be most significantly influenced by the orientation of the fibers. All fiber variables had a considerable impact on the FM, with the direction of fibers being the most crucial element. Ivan *et al.* (2022) suggests employing a data-driven inverse modeling strategy to improve the physics-based mechanical modeling of GF-reinforced plastic. By employing this method, which utilizes inverse simulation data from experiments to generate both the RSC coefficients and the RO variables, the precision of predictions for the elastic modulus increased by 43% and for the TS by 59% compared with non-optimized analysis. Muhamedagic *et al.* (2022) examines the influence of important process factors on the tensile strength of items produced by Fused Deposition Modeling (FDM). The study utilizes Response Surface Methodology (RSM) and Artificial Neural Network (ANN) to investigate the impact of the dimension, of the layer, printing acceleration, raster angle, and thickness of the wall on the TS of sample specimens created using an SCF composite. The findings demonstrate that the suggested model is a proficient tool for forecasting TS, with its main benefit being the decreased amount of experimental time needed. Deshwal *et al.* (2020) investigates the TS of Dogbone ASTM samples composed of Polylactic acid (PLA) materials. The purpose of the research is to help additive manufacturing units identify the best values for initial factors in order to produce FDM products with improved mechanical characteristics. The created hybrid models can be suggested for accurate estimation and optimization of diverse process variables and results in industrial uses.

The study revealed that the amalgamation of flax and sisal fibers yields lightweight materials with exceptional strength-to-weight ratios, rendering them well-suited for weight-sensitive applications. The study used sisal fibers intending to diminish dependence on synthetic fibers and encourage the incorporation of natural fibers into composite materials. The acknowledged the widespread usage of sisal fibers in several industries because of their strong reinforcing capabilities. They also recognized the advantages of combining flax fibers with other substances. Moreover, the study investigated how the orientation of fibers affects the improvement of the mechanical strength of these materials. The study examined the impact of different fiber orientations (0, 45, and 90 degrees) and nanoparticle inclusion on the strength of the composite material. The results showed that the varying fiber orientations and nanoparticles had a substantial effect on the strength of the composite, which supports previous research findings. The novelty of the work lies in its comprehensive investigation of fiber orientation and composition, the use of RSM and CCD for efficient experimental design, the development of predictive models, and the demonstration of significant improvements in the mechanical properties of the composites. These findings contribute to the advancement of knowledge in the field of natural fiber composite materials and provide valuable insights for the development of high-performance materials with tailored properties.

## 2. MATERIALS AND METHODOLOGY

### 2.1 Materials

The research employed a composite material that combined natural flax and sisal natural fibers to improve their characteristics in a matrix that is known for its benefits, such as strong adhesion to different types of fibers, exceptional performance at high temperatures, and excellent mechanical and electrical characteristics. The epoxy resin (LY 556) and hardener HY951 were chosen for their distinctive characteristics, including little shrinkage during the curing process and excellent chemical resistance, setting them apart from conventional thermoset polymers. Before producing the fiber plates, a sequence of controlled trials was carried out. Design Expert software was utilized to design a total of 20 experiments, with all of them having distinct fiber compositions as specified in Table 1. Fig. 1(a-e) shows Flax, Sisal fiber, Epoxy,Silicon dioxide, and Fabricated laminate. The tests established a structure for assessing different combinations of materials and their possible influence on the overall characteristics of the composite.

**Table 1. InitializationInput parameters and their levels**

| S. No. | Name | Units | L[1] | L[2] | L[3] |
|---|---|---|---|---|---|
| 1 | Fiber percentage | % | 40 | 50 | 60 |
| 2 | Fiber Orientation | Degree | 0 | 45 | 90 |
| 3 | Silicon Dioxide | % | 1 | 2 | 3 |


**Fig. 1: Materials used for the fabrication process**

## 2.2 Composite Preparation

Composite laminates spanning 300 x 300 mm were utilized to produce samples of flax and sisal nanocomposites. The samples exhibited diverse fiber orientations (0, 45, and 90 degrees) and varying fiber weight percentages (40 wt%, 50 wt%, and 60 wt%). The manufacturing procedure entailed the manual arrangement of the fibers, followed by their compression by molding techniques. The flax and sisal fibers were meticulously trimmed and organized by prescribed arrangements. A solution consisting of LY556 epoxy and HY951 hardener, mixed in a weight ratio of 10:1, was utilized and $SiO_2$ was mixed with epoxy in the mechanical stirrer method. The composites were manufactured with a uniform epoxy composition of 45% by weight. The epoxy was administered onto the surface of the fiber, subsequently subjected to compression molding, and left to cure for a single day. Following the initial curing process, the composite specimens were taken out of the steel mold and left to cure for a further 24 hours at ambient temperature. The TS and FS of the material plates were evaluated by sectioning them according to ASTM specifications using a water jet machine (WJM). As a step in the WJM process, the samples were subjected to post-curing in a hot air oven at a temperature of 65°C for 3 hours to remove any accumulated moisture (Chokshi *et al.* 2022). Table 2 presents comprehensive data regarding the different combinations employed in the creation of the hybrid composite.

**Table 2. Results from tests evaluating the TS and FS properties of nanocomposites**

| Std | Run | A:Fiber (%) | B:Fiber Orientation (Degree) | C:Silicon dioxide (%) | Tensile Strength (MPa) | Flexural Strength (MPa) |
|---|---|---|---|---|---|---|
| 1 | 15 | 40 | 0 | 1 | 53 | 71 |
| 3 | 19 | 40 | 90 | 1 | 55 | 74 |
| 13 | 4 | 50 | 45 | 1 | 61 | 81 |
| 4 | 2 | 60 | 90 | 1 | 68 | 87 |
| 2 | 1 | 60 | 0 | 1 | 69 | 89 |
| 9 | 14 | 40 | 45 | 2 | 55 | 74 |
| 16 | 11 | 50 | 45 | 2 | 62 | 82 |
| 15 | 12 | 50 | 45 | 2 | 63 | 83 |
| 17 | 13 | 50 | 45 | 2 | 64 | 84 |
| 18 | 5 | 50 | 45 | 2 | 65 | 85 |
| 19 | 9 | 50 | 45 | 2 | 65 | 85 |
| 20 | 17 | 50 | 45 | 2 | 65 | 85 |
| 10 | 3 | 60 | 45 | 2 | 66 | 85 |
| 11 | 7 | 50 | 0 | 2 | 66 | 86 |
| 12 | 8 | 50 | 90 | 2 | 67 | 87 |
| 7 | 16 | 40 | 90 | 3 | 54 | 73 |
| 5 | 20 | 40 | 0 | 3 | 56 | 76 |
| 8 | 6 | 60 | 90 | 3 | 67 | 86 |
| 14 | 18 | 50 | 45 | 3 | 67 | 87 |
| 6 | 10 | 60 | 0 | 3 | 72 | 91 |

## 2.3 Design of Experiment

The objective of this study is to utilize RSM to forecast results by analyzing the impact of different input factors on TS and FS properties. The study employs Analysis of Variance (ANOVA), a statistical technique for assessing experimental data, to determine the important impacts of fiber percentage, fiber orientation, and Nanoparticle on the ultimate technical characteristics. ANOVA enables the prioritization of input parameters according to their influence on the resultant measures. Data were gathered utilizing Design Expert V13 via a sequence of experiments, wherein ratios were determined employing an analytical experimental design methodology. The study comprised 20 tests that specifically investigated two response variables: TS and FS. The experimental design incorporated three variables: (i) the proportion of fiber, (ii) the orientation of the fibers, and (iii) Silicon dioxide %. The control parameters were set up at three levels, as seen in Table 1. Table 2 displays the findings for measures of TS and FS conducted under various testing settings. This design process facilitated a thorough analysis of how these parameters impact the effectiveness of the composite.

## 3. RESULT AND DISCUSSION

### 3.1 Evaluation of Residual and Predicted Plots for TS and FS

The residual data we have found shows a curve that closely aligns with and mirrors the observed trends in the accurate model data. The residuals shown in Fig. 2 exhibit no departures from normality. Fig. 3, shows the residual graph for a regression model. The externally studentized residuals are displayed on the y-axis, while the predicted values are represented on the x-axis. The threshold, which residuals are deemed to be outside of, is indicated by the red horizontal lines at about 4.15 and -4.15. The bulk of the residuals show a fair match between the expected and actual values, clustering around the zero line. There are a few obvious anomalies, though, especially two points that are higher than the standards for outliers. These anomalies point to possible places where the model could not function as well, indicating the need for additional research or possible model improvement.

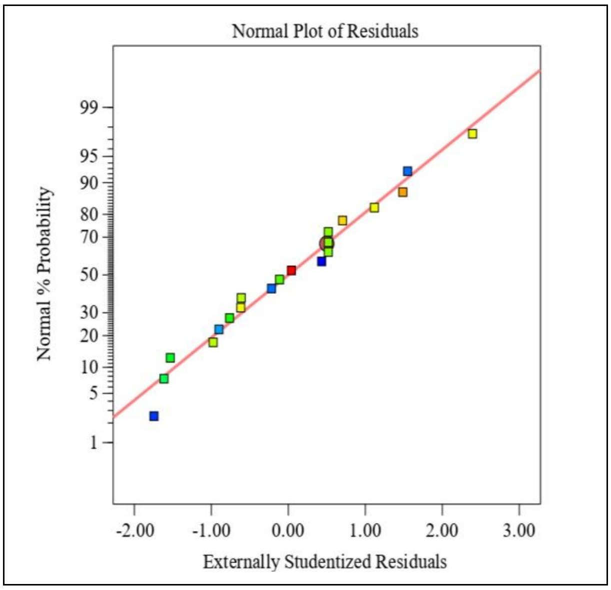


Fig. 2: Normal probability for TS

Our selected residual observation point has a robust pattern that closely corresponds with the standard data. As seen in Fig. 4, there is little to no deviation of the residual values from a normal distribution. Regression model performance is evaluated in RSM using Fig. 5. The model's predicted values are displayed on the x-axis, and the externally studentized standardized residuals that have been adjusted for variance but do not include the observation itself are displayed on the y-axis. Critical thresholds are shown by the horizontal red lines at roughly ±4.14579, and points beyond these lines may indicate probable outliers. There is little variation between the values that were observed and those that were predicted, as most of the residuals are grouped around the zero line. All things considered, the residuals' random scatter lends credence to the model's suitability and the assumption that they are normally distributed.

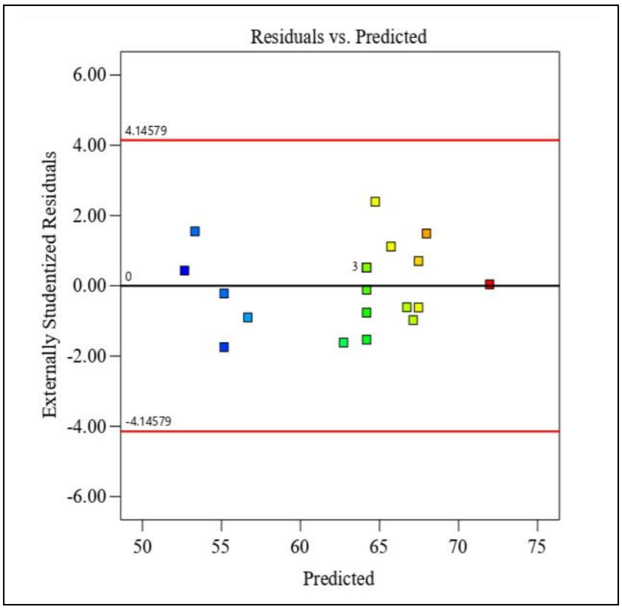


Fig. 3: Residuals vs. predicted for TS

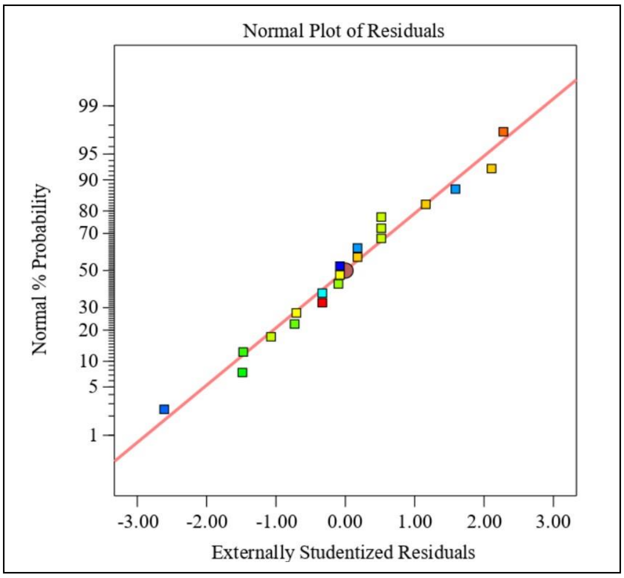


Fig. 4: Normal probability for FS

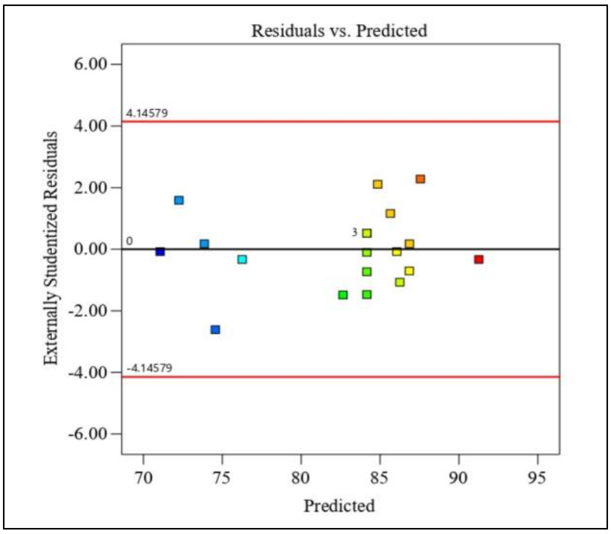


**Fig. 5: Residuals vs. predicted for FS**

## 3.2 Perturbation Plots

The TS and FS properties of the nano-composite are impacted by the fiber percentage, orientation, and $SiO_2$ loading, as shown by the graphs in Fig. 6. Based on these results, fiber orientation is the sole factor that significantly affects both TS and FS out of the three. There is a threshold beyond which higher levels in particle loading do not enhance FS but do raise the TS of the nano-composite. This is true even if the addition of Nanoparticle $SiO_2$ may improve the strength of the composite. The results found that adding more nanoparticle weight percent caused the nano-composite TS to increase, corroborating this pattern. Furthermore, even though the fiber has a high aspect ratio, the loss in FS may be explained by the excessive use of nanoparticle reinforcement, which could weaken the material's binding with the matrix. Even while $SiO_2$ nanoparticle has less of an impact than other components, it is nevertheless noticeable. The impact of its addition on TS and FS is illustrated in Fig. 6(a), where TS increases as the percentage of nanoparticles increases. As Fig. 6(b) illustrates, this trend eventually reverses, resulting in a further rise in flexural strength. Increased filler content has the potential to significantly delignify native fiber, weakening and increasing its susceptibility. Consistent with our finding that the best Nano-filler concentration results in outstanding mechanical characteristics.

The p-values and f-values from the ANOVA analysis ($f=23.77$, $p<0.0001$) are shown in Table 3 and support the validity of the suggested model. The linear terms (A, B, C), interaction terms (AB, BC, AC), and quadratic terms ($A^2$, $B^2$, $C^2$) in the model are evaluated based on these values. With p-values of less than 0.0001, and less than 0.001 A, $A^2$, and $B^2$ are all highly significant. The model's validity is shown by the little, less than 0.2 difference between the adjusted TS estimated with $R^2$ and the anticipated TS derived with $R^2$. Equation 1 provides additional evidence for the quantitative model's adequacy. Three-dimensional illustrations that depict how various process variables and TS relate to one another are shown in Figure 7. The figures show regular trends in the TS fluctuations that are impacted by various combinations of process factors, including the percentages of fiber percentage, Fiber orientation, and silicon dioxide. TS and the amount of $SiO_2$ in the hybrid nanocomposite are directly correlated, as seen in Fig. 7(a), which also highlights the effect of $SiO_2$ on the ratios of fiber percentage and orientation. Furthermore, the strength of the composite is greatly increased by the nanoparticles present in the fibers. More specifically, an important enhancement in the material's characteristics is noted with 3% $SiO_2$ with fiber 60% and Fiber orientation of 0 degrees of the material.

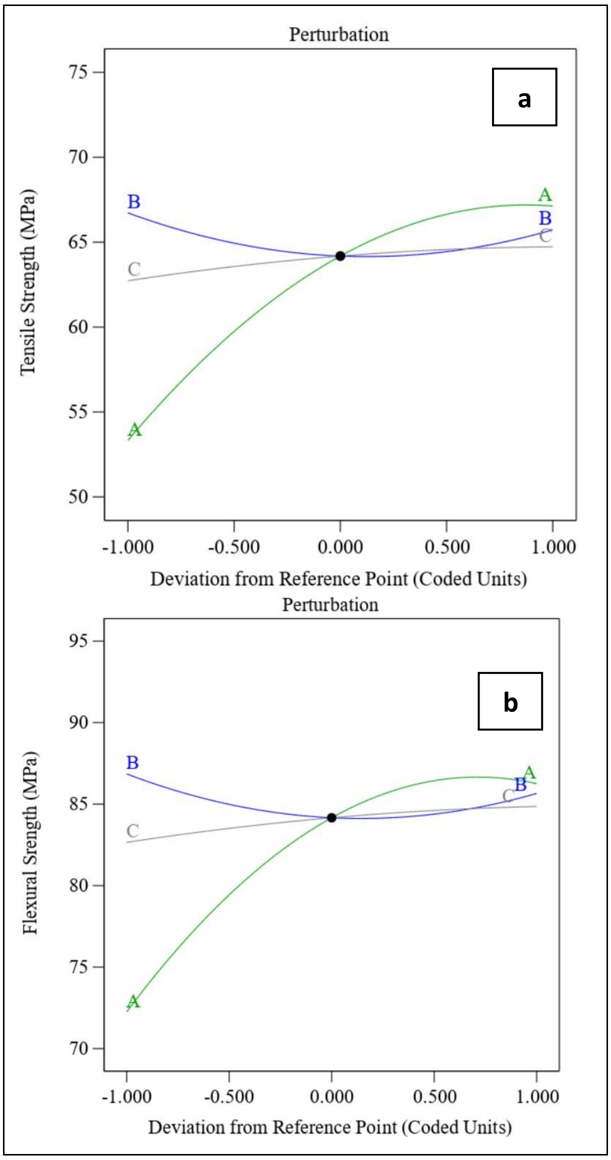


**Fig. 6: Perturbation Plots (a) TS and (b) FS**

**Table 3. ANOVA for TS**

| Source | Sum of Squares | df | Mean Square | F-value | p-value | |
|---|---|---|---|---|---|---|
| **Model** | 557.92 | 9 | 61.99 | 23.77 | < 0.0001 | significant |
| A-Fiber | 476.10 | 1 | 476.10 | 182.54 | < 0.0001 | |
| B-Fiber Orientation | 2.50 | 1 | 2.50 | 0.9585 | 0.3507 | |
| C-Silicon dioxide | 10.00 | 1 | 10.00 | 3.83 | 0.0787 | |
| AB | 4.50 | 1 | 4.50 | 1.73 | 0.2183 | |
| AC | 0.0000 | 1 | 0.0000 | 0.0000 | 1.0000 | |
| BC | 8.00 | 1 | 8.00 | 3.07 | 0.1104 | |
| $A^2$ | 43.01 | 1 | 43.01 | 16.49 | 0.0023 | |
| $B^2$ | 11.51 | 1 | 11.51 | 4.41 | 0.0620 | |
| $C^2$ | 0.5682 | 1 | 0.5682 | 0.2178 | 0.6507 | |
| **Residual** | 26.08 | 10 | 2.61 | | | |
| Lack of Fit | 18.08 | 5 | 3.62 | 2.26 | 0.1958 | not significant |
| Pure Error | 8.00 | 5 | 1.60 | | | |
| **Cor Total** | 584.00 | 19 | | | | |

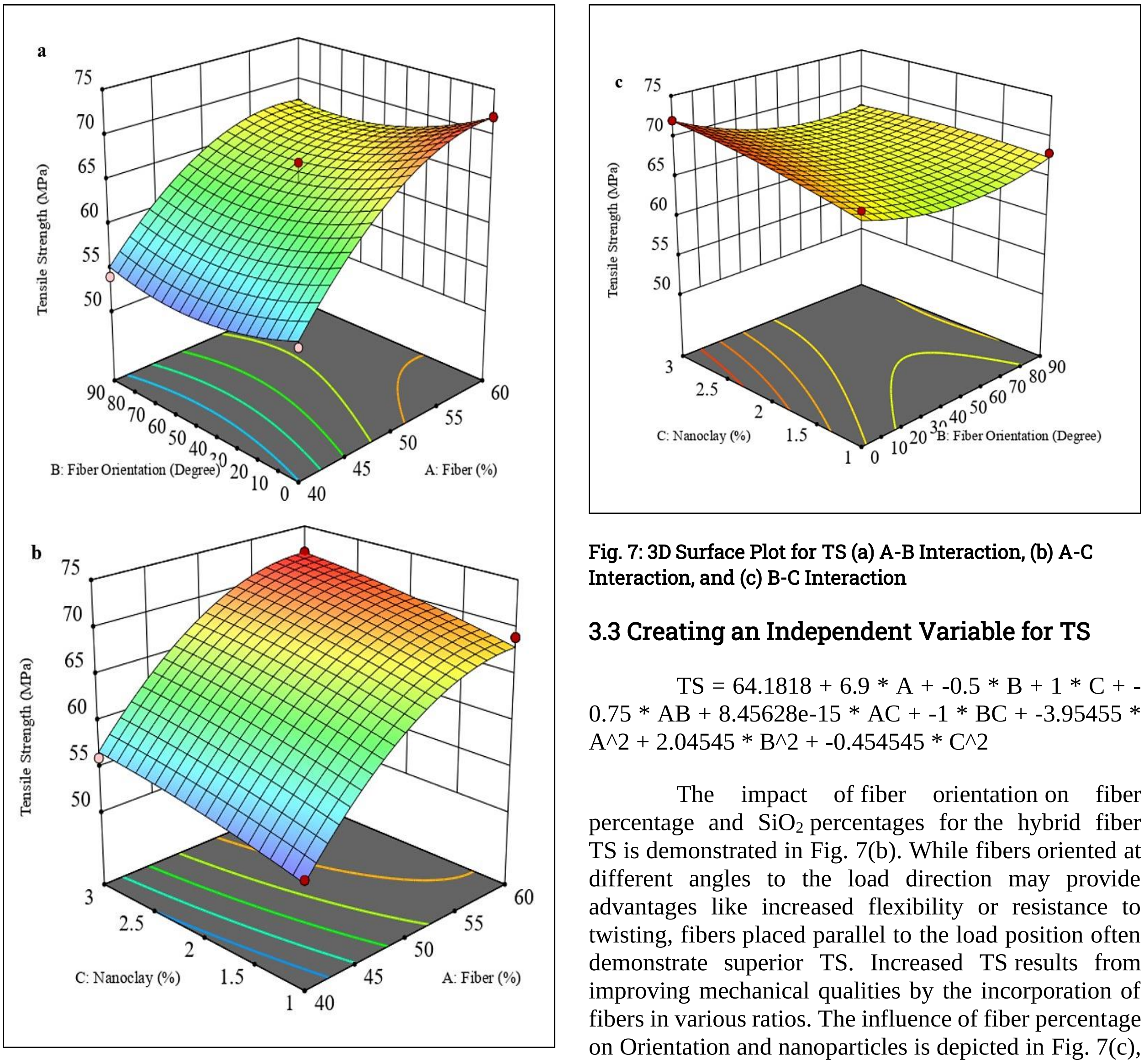


**Fig. 7: 3D Surface Plot for TS (a) A-B Interaction, (b) A-C Interaction, and (c) B-C Interaction**

## 3.3 Creating an Independent Variable for TS

TS = 64.1818 + 6.9 * A + -0.5 * B + 1 * C + -0.75 * AB + 8.45628e-15 * AC + -1 * BC + -3.95455 * A^2 + 2.04545 * B^2 + -0.454545 * C^2

The impact of fiber orientation on fiber percentage and $SiO_2$ percentages for the hybrid fiber TS is demonstrated in Fig. 7(b). While fibers oriented at different angles to the load direction may provide advantages like increased flexibility or resistance to twisting, fibers placed parallel to the load position often demonstrate superior TS. Increased TS results from improving mechanical qualities by the incorporation of fibers in various ratios. The influence of fiber percentage on Orientation and nanoparticles is depicted in Fig. 7(c), emphasizing the relationship between orientation and $SiO_2$ in strengthening resilience. The proportions and fiber alignment also play a significant role in defining the properties of the composite. These results offer important new understandings of the intricate connection between different fiber kinds, their orientations, and the material strength that results.

### 3.4 Creating an independent variable for FS

FS = 84.1636 + 7 * A + -0.6 * B + 1.1 * C + -0.875 * AB + -0.375 * AC + -1.125 * BC + -4.90909 * A^2 + 2.09091 * B^2 + -0.409091 * C^2.

**Table 4. ANOVA for FS**

| Source | Sum of Squares | df | Mean Square | F-value | p-value | |
|---|---|---|---|---|---|---|
| **Model** | 611.60 | 9 | 67.96 | 24.84 | < 0.0001 | significant |
| A-Fiber | 490.00 | 1 | 490.00 | 179.14 | < 0.0001 | |
| B-Fiber Orientation | 3.60 | 1 | 3.60 | 1.32 | 0.2780 | |
| C-Silicon dioxide | 12.10 | 1 | 12.10 | 4.42 | 0.0617 | |
| AB | 6.13 | 1 | 6.13 | 2.24 | 0.1654 | |
| AC | 1.13 | 1 | 1.13 | 0.4113 | 0.5357 | |
| BC | 10.13 | 1 | 10.13 | 3.70 | 0.0833 | |
| $A^2$ | 66.27 | 1 | 66.27 | 24.23 | 0.0006 | |
| $B^2$ | 12.02 | 1 | 12.02 | 4.40 | 0.0624 | |
| $C^2$ | 0.4602 | 1 | 0.4602 | 0.1683 | 0.6903 | |
| **Residual** | 27.35 | 10 | 2.74 | | | |
| Lack of Fit | 19.35 | 5 | 3.87 | 2.42 | 0.1772 | not significant |
| Pure Error | 8.00 | 5 | 1.60 | | | |
| **Cor Total** | 638.95 | 19 | | | | |

As demonstrated in Table 4, the F-value of 24.84 and a p-value of less than 0.0001 strongly suggest that the CCD-RSM approach is a particularly suitable model for forecasting FS. P-values for each of the process indicators (A, A2, and B2) are less than 0.05. Process factors consistently have an impact on FS, as demonstrated by the substantial p-values derived from the observational data and the little discrepancy between the adjusted $R^2$ and anticipated $R^2$ values, all of which coincide within 0.2. These results provide additional evidence for the correctness of the mathematical framework used in Equation 2.

Figure 7 shows the FS as a three-dimensional curve that highlights the consequences of different configurations using a three-dimensional surface plot. Fig. 8(a) shows that there is a discernible rise in the interaction pattern between the fiber percentage and fiber orientation. Further information on the correlations between variations in the fiber percentage and $SiO_2$ is given in Fig. 8(b). The influence of fiber orientation and $SiO_2$ is depicted in Fig. 8(c), which demonstrates how $SiO_2$ increases the resilience of the nano-composite. These results provide strong evidence that biodegradable flax and sisal fiber is becoming more and more important across a range of industrial industries. Applying $SiO_2$ particles greatly enhances mechanical qualities, according to a comprehensive analysis of several factors. Superior strength is achieved by the unique structure, which uses a 60% weight percentage of fibers and 3% $SiO_2$, and 0-degree fiber orientation. When compared to other variables that were investigated with RSM, this combination produces a higher value.

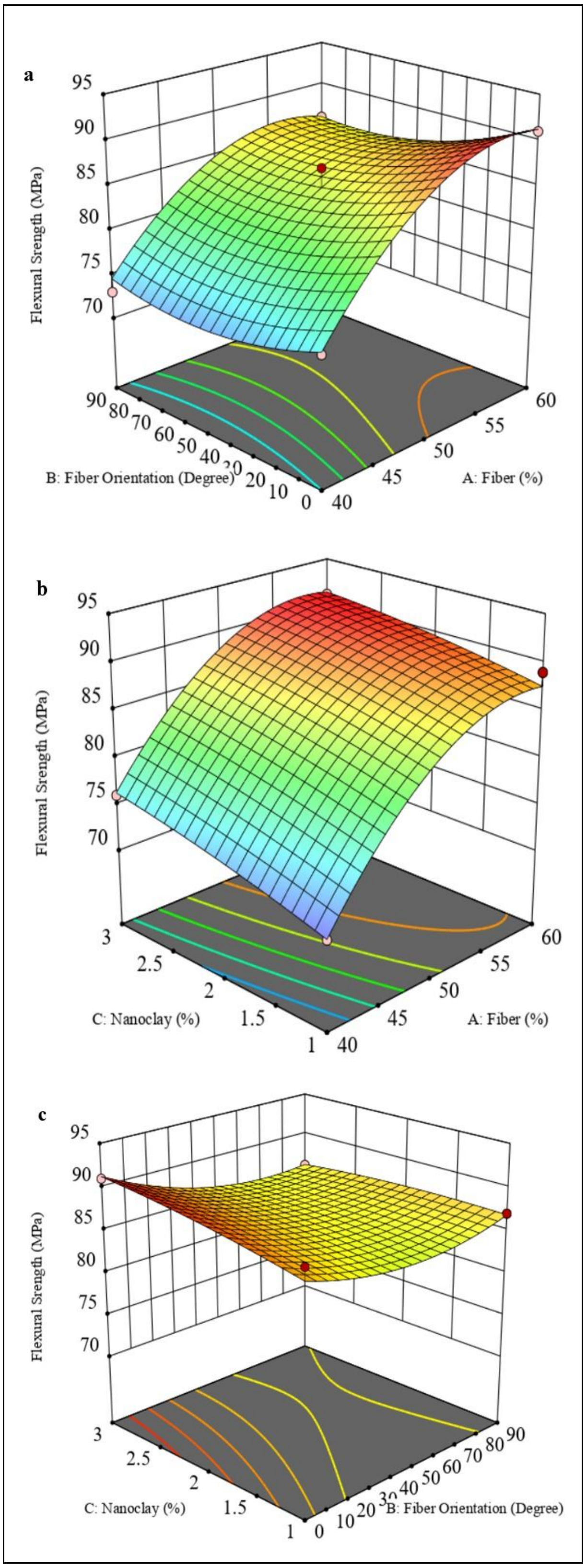


Fig. 8: 3D Surface Plot for FS (a) A-B Interaction, (b) A-C Interaction, and (c) B-C Interaction

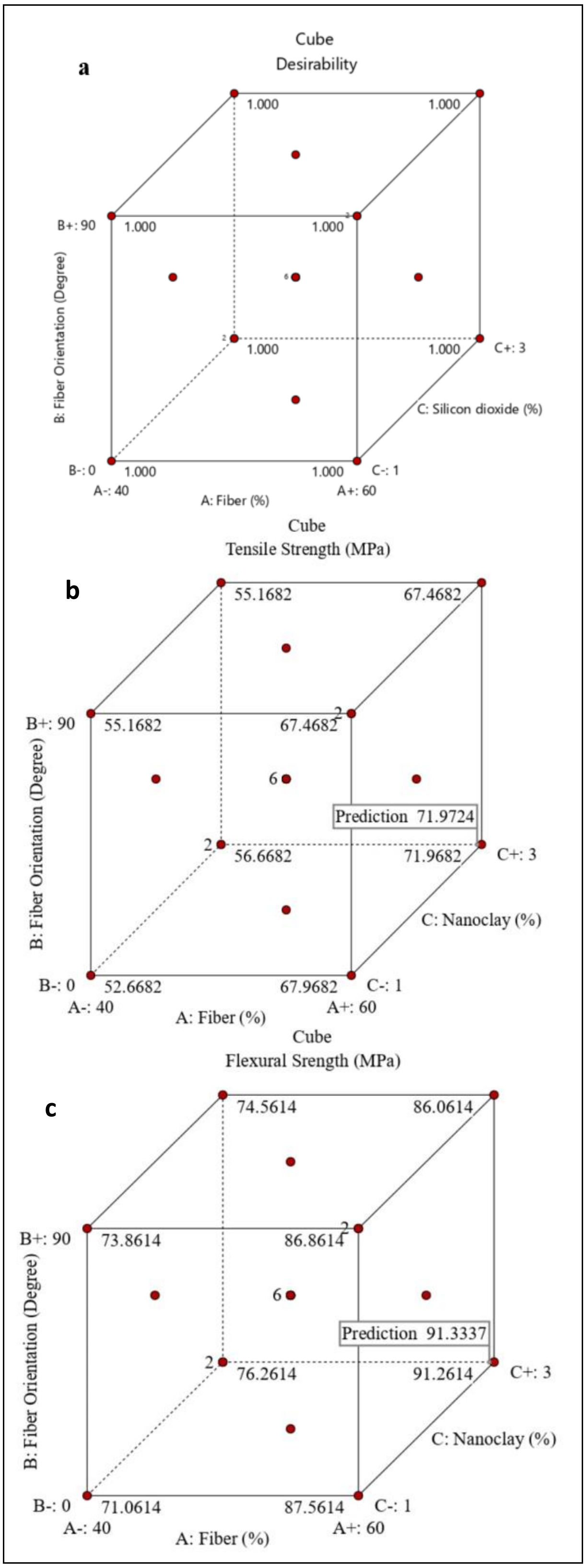


Fig. 9: Cube Plot (a) Desirability, (b) TS, and (c) FS

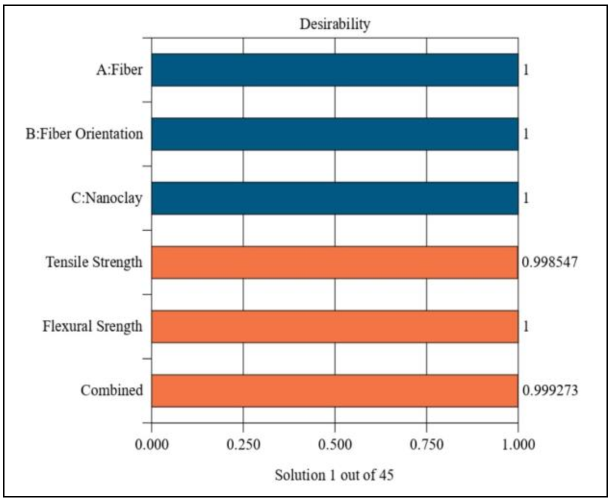


**Fig. 10: Depicts the desirability solution plot**

### 3.5 Cube Plot

Cube plots are presented in Fig. 9, which provide a concise summary of the dynamics of mechanical features. These cube plots clearly illustrate the interactions that occur between the various components and levels. It was shown that increasing the number of nanoparticles and modifying the fiber percentage increased TS and FS. Moreover, there was a substantial increase in desirability, 1.000 whenever there was a rise in the amount of nanoparticle contained. The pattern that has been observed suggests that there is a positive association between TS and FS characteristics including the orientation of the fibers, fibers percentage, and the amount of nanoparticles. It is possible to achieve a cubic depiction with a desired value of 1, as shown in Fig. 9(a), by ensuring that the fibers are oriented and fiber percentage precisely measured, as well as by using nanoparticles at a weight percentage of 3 percent. In addition, the cube plots shown in Fig. 9(b) demonstrate that the greatest TS of 71.96 MPa was produced by utilizing a fiber orientation of 0 degrees and a nanoparticle percentage of 3 weight percent. An illustration of a cubic model depiction with an FS value of 91.26 MPa is shown in Fig. 9(c). This model is characterized by 0-degree fiber orientation, 60 Fiber percentage, and a nanoparticle of 3 weight percent $SiO_2$.

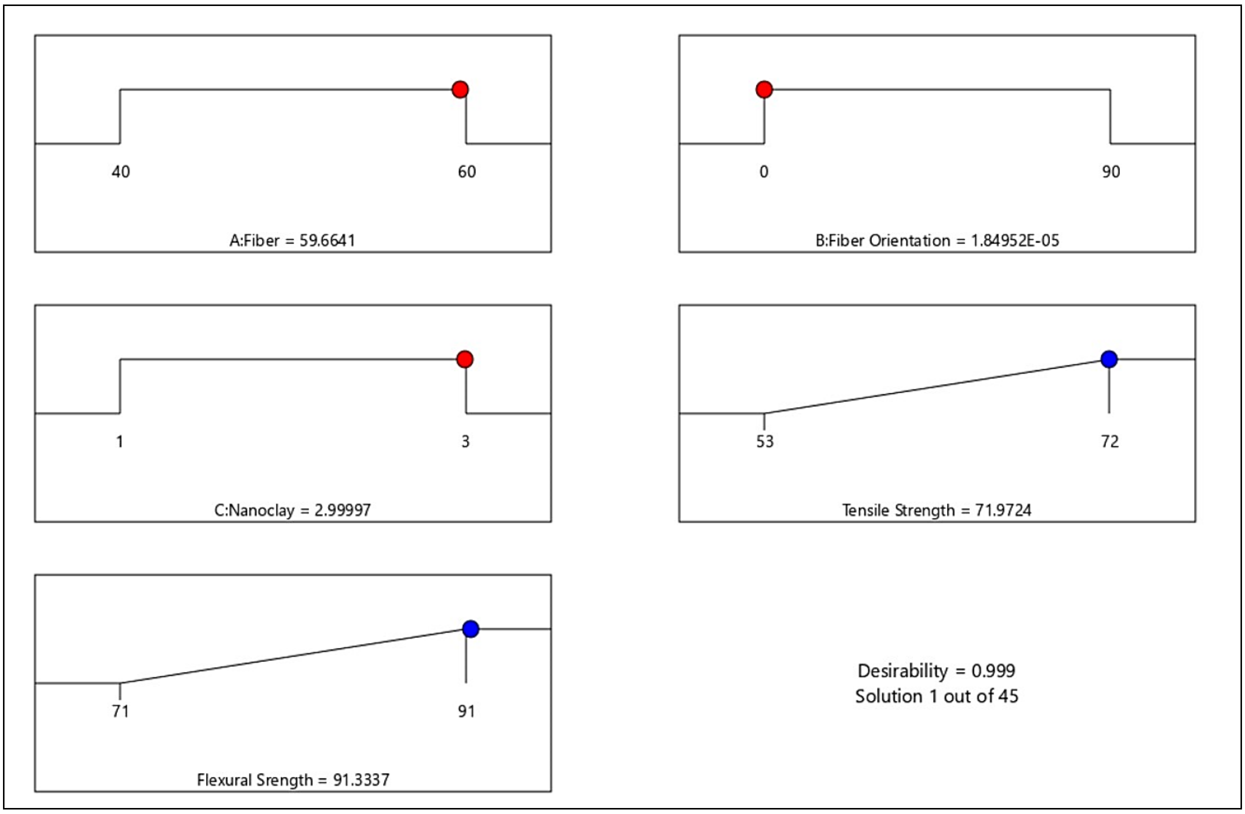


**Fig. 11: Ramp functional graph**

### 3.6 Ramp Functional Graph

The desirability plot depicted in Fig. 10 illustrates the optimization of various parameters for the composite material. Fiber type (A), fiber orientation (B), and silicon dioxide content (C) are the criteria that are being considered. Each of these factors has a desirability value of 1, which indicates that the conditions are ideal. The individual replies for tensile strength and flexural strength are likewise displayed, with desirability values of 0.998547 and 1, respectively, for each of these strengths. Given that the total configuration of these parameters yields results that are close to ideal for both tensile and flexural strengths, the combined desirability score of 0.999273 indicates that this configuration is desirable. The efficiency of the model in optimizing the mechanical properties of the nanocomposite is demonstrated by the high level of attractiveness that it possesses. After a thorough investigation of the factors influencing the tensile Strength and flexural strength of nanocomposites, we have identified the optimal parameter ranges for enhancing these properties. Our research indicates that the most advantageous range for achieving peak tensile strength is between 53 and 72 MPa. The ideal range for flexural strength lies between 71 and 91. Fig. 11 visually outlines our optimization process, highlighting the most effective operational conditions for maximizing both the tensile and flexural strength of the nanocomposite. These optimal conditions involve using a 3% concentration of silicon dioxide nanoparticles, aligning the fibers at a 0-degree angle, and following a fiber percentage of 60. To validate the scientific rigor of our findings, we conducted impact experiments under these optimized conditions. The results of these experiments showed an exceptionally high level of agreement, with nearly 100% correspondence to the predicted values generated by our model, similar to the outcomes. This strong consistency between the anticipated results and the actual experimental values serves as robust validation, confirming the practicality and effectiveness of the optimized settings we have identified.

## 4. CONCLUSION

The research investigated the effective production of hybrid polymer composites that contained $SiO_2$ fillers. The primary objective of the investigation was to predict the tensile strength and flexural strength of these composites based on three variables that were present at various factors. To plan experimental setups and conduct analyses of response surfaces, perturbation plots, cube plots, and desirability functions through RSM application were utilized. The built regression models demonstrated a high level of precision, with a 95% accuracy rate, which indicates that they are reliable in predicting composite features. The combination of natural fibers with $SiO_2$ nanoparticles, which were found to be important factors influencing TS and FS, was a significant innovation that was implemented inside the material. According to the findings of the research, increasing the amount of $SiO_2$ in the material increased tensile strength by up to 72 MPa and 92 MPa for flexural strength. Additionally, precise fiber percentage and orientations had a substantial impact on TS and FS. In comparison to the other configurations that were investigated, the experimental runs that were conducted with 3% $SiO_2$ at a 0-degree angle, and 60 % fiber demonstrated significant gains in TS and FS.

## REFERENCES


Arunachalam, S. J., Saravanan, R., Sathish, T. and Parthiban, A., Effect of nano-particle weight percent on the flexural strength of Jute/kenaf/glass fiber composite using RSM, *Interactions*, 245(1), 83 (2024). https://doi.org/10.1007/s10751-024-01920-2

Arunachalam, S. J., Saravanan, R., Sathish, T. and Parthiban, A., Comprehensive insights on mechanical properties of natural-synthetic fibres with nano-graphene composite, *Interactions*, 245(1), 82 (2024). https://doi.org/10.1007/s10751-024-01921-1

Benzannache, N., Belaadi, A., Boumaaza, M. and Bourchak, M., Improving the mechanical performance of biocomposite plaster/Washingtonian filifira fibres using the RSM method, *J. Build. Eng.*, 33, 101840 (2021). https://doi.org/10.1016/j.jobe.2020.101840

Chang, B., Gu, J., Long, Z., Li, Z., Ruan, S. and Shen, C., Effects of temperature and fiber orientation on the tensile behavior of short carbon fiber reinforced PEEK composites, *Polym. Compos.*, 42(2), 597-607 (2021). https://doi.org/10.1002/pc.25850

Chokshi, S., Parmar, V., Gohil, P. and Chaudhary, V., Chemical composition and mechanical properties of natural fibers, *J. Nat. Fibers.*, 19(10), 3942-3953 (2022). https://doi.org/10.1080/15440478.2020.1848738

Cordin, M., Bechtold, T. and Pham, T., Effect of fibre orientation on the mechanical properties of polypropylene–lyocell composites, *Cellulose*, 25, 7197-7210 (2018). https://doi.org/10.1007/s10570-018-2079-6

Deshwal, S., Kumar, A. and Chhabra, D., Exercising hybrid statistical tools GA-RSM, GA-ANN and GA-ANFIS to optimize FDM process parameters for tensile strength improvement, *CIRP J. Manuf. Sci. Technol.*, 31, 189-199 (2020). https://doi.org/10.1016/j.cirpj.2020.05.009

Huang, H., Gao, X. and Teng, L., Fiber alignment and its effect on mechanical properties of UHPC: An overview, *Constr Build Mater.*, 296, 123741 (2021). https://doi.org/10.1016/j.conbuildmat.2021.123741

Iliyasu, I., Bello, J. B., Dibal, M. N., Oyedeji, A. N., Salami, K. A. and Oyedeji, E. O., Response surface methodology for the optimization of the effect of fibre parameters on the physical and mechanical properties of deleb palm fibre reinforced epoxy composites, *Sci. Afr.*, 16, e01269 (2022). https://doi.org/10.1016/j.sciaf.2022.e01269

Ivan, R., Sorgato, M., Zanini, F. and Lucchetta, G., Improving numerical modeling accuracy for fiber orientation and mechanical properties of injection molded glass fiber reinforced thermoplastics, *Materials*, 15(13), 4720 (2022). https://doi.org/10.3390/ma15134720

Jothi Arunachalam, S., Saravanan, R., Sathish, T., Haider, S. and Giri, J., Investigation of chemically treated jute/kenaf/glass fiber with $TiO_2$ nano-filler for tensile and impact characteristics, *AIP Advances*, 14(4), 045133 (2024). https://doi.org/10.1063/5.0206141

Manral, A., Singh, R., Ahmad, F., Das, P. P., Chaudhary, V., Joshi, R. and Srivastava, P., Multi-objective optimization of mechanical properties of chemically treated bio-based composites using response surface methodology, *Compos. Part C: Open Access.*, 10, 100337 (2023). https://doi.org/10.1016/j.jcomc.2022.100337

Mohd Nurazzi, N., Khalina, A., Chandrasekar, M., Aisyah, H. A., Ayu Rafiqah, S., Ilyas, R. A. and Hanafee, Z. M., Effect of fiber orientation and fiber loading on the mechanical and thermal properties of sugar palm yarn fiber reinforced unsaturated polyester resin composites, *Polimery*, 65(2), 115–124 (2020). https://doi.org/10.14314/polimery.2020.2.5

Muhamedagic, K., Berus, L., Potočnik, D., Cekic, A., Begic-Hajdarevic, D., Cohodar Husic, M. and Ficko, M., Effect of process parameters on tensile strength of FDM printed carbon fiber reinforced polyamide parts, *Appl. Sci.*, 12(12), 6028 (2022). https://doi.org/10.3390/app12126028

Nugroho, G. and Budiyantoro, C., Optimization of fiber factors on flexural properties for carbon fiber reinforced polypropylene, *J. Compos. Sci.*, 6(6), 160 (2022). https://doi.org/10.3390/jcs6060160

Rangasamy, G., Mani, S., Kolandavelu, S. K. S., Alsoufi, M. S., Ibrahim, A. M. M., Muthusamy, S. and Elsheikh, A. H., An extensive analysis of mechanical, thermal and physical properties of jute fiber composites with different fiber orientations, *Case Stud. Therm. Eng.*, 28, 101612 (2021). https://doi.org/10.1016/j.csite.2021.101612

Saravanakumar, S., Sathiyamurthy, S., Pathmanaban, P. and Devi, P., Integrating machine learning and response surface methodology for analyzing anisotropic mechanical properties of biocomposites, *Compos Interfaces*, 31(1), 1-28 (2024). https://doi.org/10.1080/09276440.2023.2260239

Van De Werken, N., Reese, M. S., Taha, M. R. and Tehrani, M., Investigating the effects of fiber surface treatment and alignment on mechanical properties of recycled carbon fiber composites, *Compos. - A: Appl. Sci. Manuf.*, 119, 38-47 (2019). https://doi.org/10.1016/j.compositesa.2019.01.012

Zhang, W. and He, C., Investigation and prediction of mechanical properties of hot water treated jute/poly (lactic acid) composite laminates using response surface methodology and genetic algorithm, *Polym. Compos.*, 43(10), 7170-7186 (2022). https://doi.org/10.1002/pc.26780